TWIN-BEAM LASER VELOCIMETER FOR THE INVESTIGATION OF SPERMATOZOON MOTILITY

M. C. WILSON AND J. D. HARVEY
Physics Department, University of Auckland, Private Bag, Auckland, New Zealand

ABSTRACT Previous laser light-scattering studies of spermatozoon motility have been hampered by the large, asymmetric shape of spermatozoa, which causes difficulties in the interpretation of intensity fluctuations in the light scattered from a single laser beam. This paper describes an experimental arrangement for measuring the distribution of transit times for swimming spermatozoa using two slightly separated, focused laser beams. The theory of operation of the instrument is developed to enable the analysis of the experimentally obtained cross-correlation functions. The effects of the pronounced spermatozoon asymmetry and associated intensity modulation in the scattered light are also investigated and shown to be negligible for the twin beam experimental arrangement, provided that the swimming speed distribution has a coefficient of variation $(\sigma/\bar{v}) > 0.1$. Results obtained using this apparatus are presented for the velocity distribution of spermatozoa from a variety of bulls.

INTRODUCTION

The study of the intensity fluctuations of laser light scattered from swimming spermatozoa dates from the early paper by Bergé et al. 1967, in which it was shown that the spectrum of these fluctuations was broader for motile cells than for immotile cells (for a review of subsequent work in this field see Cummins, 1977 and references therein). This result is to be expected if the cells are modeled as Doppler scatterers, and many studies have attempted to extract the velocity distribution of the swimming cells from the spectrum or autocorrelation function of the scattered light intensity. The modeling of the sperm cell as a point scattering center, however, is a gross approximation with varying consequences that depend upon the particular shape of the cells studied. In the case of bull spermatozoa and other cells that are large and flat (when compared with the wavelength of light) such an analysis is completely inadequate because the scattered light seen by the detector arises almost totally from the cells swimming in a direction perpendicular to the scattering vector and the intensity fluctuations in the scattered light depend only upon the rotational frequency of the swimming cells (Craig et al., 1979. Harvey and Woolford, 1980). This phenomenon (which also occurs with other mammalian cells, notably ram spermatozoa) enables the rotational frequency of the cells to be extracted from the spectrum of the intensity fluctuations if the swimming motion is adequately modeled in the theory, and this may well be a useful measure of the vigor of the swimming population.

To ascertain whether the rotational frequency is a good indication of the translational speed, a different method of measuring the distribution of translational velocities is required. Furthermore, it is desirable to measure this distribution by laser light scattering because the method promises rapid reliable analysis by a nonperturbative technique and has undergone considerable development in the decade following its first application. This paper describes a method of direct measurement of the velocity distribution by use of scattered light from a twin beam laser apparatus, the transit time laser velocimeter (TTLV). As an anemometer this instrument has received considerable attention in recent years as it offers a marked improvement in flare reduction over the laser Doppler velocimeter (LDV) (see for example Schodl, 1976; Lading, 1976; Kugler, 1979; and Durrani and Greated, 1975). In the experiments reported here the TTLV was preferred to the LDV because of the difficulty in interpreting the intensity fluctuations in light scattered from motile bull spermatozoa. For a population of cells moving in random directions the transit time velocimeter provides good velocity resolution, and in the limit of very small beams it provides an unambiguous measurement of the swimming speed distribution for a sample whose scattered light can also be analyzed by the common single-beam intensity fluctuation method, and it may be used to investigate the shortcomings of this latter method.

THEORY

The ideal transit time velocimeter consists of two infinitesimally narrow parallel beams separated by a distance d. Light will be scattered from particles as they traverse the beams; by separating the scattered light into components originating in separate beams and cross-correlating their intensities it is possible to recover the distribution of transit times of the particles between the beams, $p(\tau)$. Indeed, as shown by Durrani and

Greated (1977) the cross-correlation between the intensities is

$$R(\tau) = I_0^2 \sum_{\substack{i \\ i \neq j}} \sum_{j} \text{probability } (i\text{th scatterer arrives at the first beam at time } t \text{ and } j\text{th scatterer at the second beam at } t + \tau)$$

$$+ I_0^2 \sum_{i} \text{probability } (i\text{th scatterer arrives at the first beam at } t \text{ and then at the second beam at } t + \tau)$$

$$= I_0^2 N_p^2 + I_0^2 N_p p(\tau) \tag{1}$$

where N_P is the mean number of arrivals per second.

Under suitable experimental conditions it is possible to recover the distribution of swimming speeds from the distribution of transit times. It is necessary to restrict the motion of the particles to a direction perpendicular to the beam axes. This restriction can be satisfied for dust particles suspended in a laminar flow by suitably directing the flow while it can be achieved for motile spermatozoa by suitably designing the experimental apparatus (see Methods). Those particles that traverse both beams will then have travelled the same distance d between beam encounters, and the distribution of swimming speeds, $p(v)$, can thereby be found using Eq. 1 (see Papoulis, 1965):

$$p(v) = \left| \frac{d\tau}{dv} \right| p(\tau)$$

$$= \frac{\tau^2}{d} p(\tau)$$

$$= \frac{\tau^2}{d} \left(\frac{R(\tau)}{I_0^2 N_p} - N_p \right). \tag{2}$$

Eq. 2 is exact in the case of point scatterers which move through beams that are very much narrower than the distance between the beam centers. Any real transit-time laser velocimeter, however, must consist of beams of appreciable width. Consequently the correlation function of Eq. 1 will be homogeneously broadened as a result of the particles' finite passage time across the beams and inhomogeneously broadened, with a bias towards shorter transit times, as a consequence of those particles whose trajectories are inclined at an angle to the direct path between the beam centers. These effects are considered in detail in the following sections. The cross-correlation function is evaluated first for a point scatterer travelling between laser beams of finite width and Gaussian intensity profile.

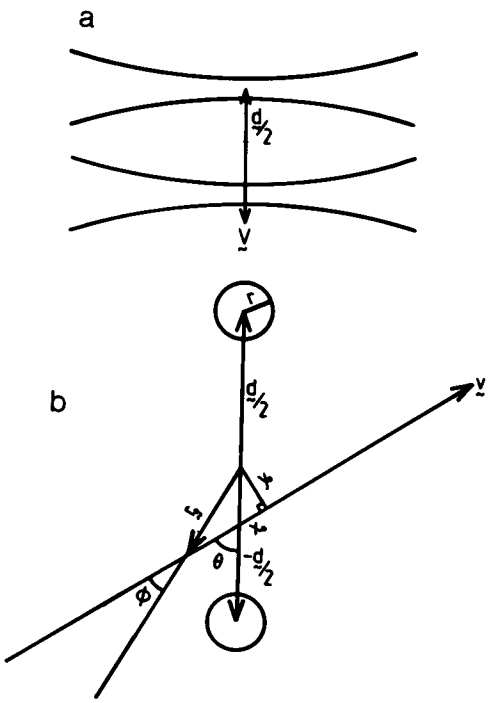

FIGURE 1 (*a*) Top view of the transit-time laser velocimeter. Particle trajectories are confined to the plane that is perpendicular to the beam axes and passes through the beam waists. (*b*) End view of the transit-time laser velocimeter showing a typical particle trajectory. The origin of the coordinate system is taken to be the centre between the beam waists.

Single-Particle Cross-Correlation Function

The intensity distributions of two parallel beams from a laser operating in its fundamental mode are

$$I_i(\mathbf{x}) = \frac{2P_{0i}}{\pi r^2} \exp - \frac{2}{r^2} \left| \mathbf{x} \pm \frac{\mathbf{d}}{2} \right|^2, \quad i = 1, 2$$

where r is the beam radius to the $1/e^2$ points of beam intensity and P_{0i} is the ith beam power.

Suppose that a point scatterer passes close to the beams in a plane perpendicular to the beam axes with velocity $\mathbf{v}$ and trajectory $\mathbf{x} = \mathbf{v}t + \mathbf{r}_0$ (see Fig. 1). Then the intensities scattered by it are:

$$I_{is}(t) \propto I_i[x(t)] = \frac{2P_{0i}}{\pi r^2} \exp - \frac{2}{r^2} \left| \mathbf{v}t + \mathbf{r}_0 \pm \frac{\mathbf{d}}{2} \right|^2, \quad i = 1, 2.$$

The cross-correlation between the scattered intensities is therefore

$$R_{\text{point}}(\tau) = \langle I_{1s}(t) I_{2s}(t + \tau) \rangle$$

$$\propto \frac{1}{r^4} \int_{-\infty}^{\infty} dt \exp - \frac{2}{r^2} \left[\left| \mathbf{v}t + \mathbf{r}_0 + \frac{\mathbf{d}}{2} \right|^2 + \left| \mathbf{v}(t + \tau) + \mathbf{r}_0 - \frac{\mathbf{d}}{2} \right|^2 \right]$$

$$= \frac{\sqrt{\pi}}{2vr^3} \exp - \frac{1}{r^2} [|\mathbf{v}\tau - \mathbf{d}|^2 + 4 r_0^2 \sin^2 \phi] \tag{3}$$

$$= \frac{\sqrt{\pi}}{2vr^3} \exp - \frac{1}{r^2} [(v\tau - d \cos \theta)^2 + d^2 \sin^2 \theta + 4r_0^2 \sin^2 \phi] \tag{4}$$

where θ is the angle between $\mathbf{v}$ and $\mathbf{d}$ and ϕ is the angle between $\mathbf{v}$ and $\mathbf{r}_0$. $x_0 = r_0 \cos \phi$ is therefore the initial distance of the particle from its point of closest approach to the beams' center and $y_0 = r_0 \sin \phi$ is the distance of closest approach to the beams' center. The distances of closest approach to each individual beam center are $d \sin \theta \pm r_0 \sin \phi$. Clearly those particles passing closer to the beam centers will give rise to larger cross-correlations and this is expressed in the factor $\exp - (d^2 \sin^2 \theta + 4r_0^2 \sin^2 \phi)/r^2$.

The cross correlation function from a single particle thus takes the form of a Gaussian centred at

$$\tau_{\text{peak}} = \frac{\text{beam separation in direction of } \mathbf{v}}{\text{speed}}$$

$$= \frac{d \cos \theta}{v}.$$

The transit time is greatest for the particles that move directly through the beam centers and falls off as their direction (θ) becomes more oblique. Furthermore, the magnitude of the cross-correlation function diminishes as θ increases.

The effect of the finite beam width is to broaden the cross-correlation peak by an amount r/v. This is analogous to the so-called Doppler broadening that occurs in LDV.

Many Particle Cross-Correlation Function

Suppose that an ensemble of motile micro-organisms of negligible size and varying velocity passes through the TTLV. The cross-correlation function of the scattered light will be an average of Eq. 3 over velocity, $\mathbf{v}$, and initial position, $\mathbf{r}_0 = (x_0, y_0) = r_0(\cos\phi, \sin\phi)$:

$$\langle R_{\text{point}}(\tau)\rangle = \frac{\sqrt{\pi}}{2r^3}\int\int d\mathbf{r}_0\, d\mathbf{v}\, p(\mathbf{v})\frac{1}{v}\exp -\frac{1}{r^2}$$
$$[|\mathbf{v}\tau - \mathbf{d}|^2 + 4r_0^2\sin^2\phi]$$
$$= \frac{\sqrt{\pi}}{2r^3}\int d\mathbf{v}\, p(\mathbf{v})\int_{-v\tau}^{v\tau} dx_0\int_{-\infty}^{\infty} dy_0\frac{1}{v}\exp -\frac{1}{r^2}$$
$$[|\mathbf{v}\tau - \mathbf{d}|^2 + 4y_0^2]$$
$$= \frac{\pi T}{2r^2}\int d\mathbf{v}\, p(\mathbf{v})\exp -\frac{1}{r^2}|\mathbf{v}\tau - \mathbf{d}|^2 \qquad (5)$$
$$= \frac{\pi T}{2r^2}\int_0^{\infty}\int_0^{2\pi} v\,dv\,d\theta\, p(v)p(\theta)\exp$$
$$-\frac{1}{r^2}(v^2\tau^2 - 2vd\tau\cos\theta + d^2). \qquad (6)$$

where $p(v)$ is the distribution of particle speeds, $p(\theta)$ is the distribution of directions and T is the duration of the experiment.

For isotropic swimmers moving in random directions $p(\theta) = (2\pi)^{-1}$ and hence

$$\langle R_{\text{point}}(\tau)\rangle_{\text{random}} = \frac{\pi T}{2r^2}\int_0^{\infty} dv p(v)v\exp\frac{-1}{r^2}$$
$$\{v^2\tau^2 + d^2\}\int_0^{2\pi} d\theta\left(\frac{1}{2\pi}\right)\exp\frac{(2vd\tau\cos\theta)}{r^2}$$
$$= \frac{\pi T}{2r^2}\int_0^{\infty} dv p(v)v\exp -\frac{1}{r^2}\{v^2\tau^2 + d^2\}I_0\left(\frac{2vd\tau}{r^2}\right)$$
$$= R_{\text{random}}(\tau) \qquad (7)$$

where $I_0(x)$ is the zeroth-order modified Bessel function of the first kind.

In comparison, those particles that are suspended in a flow have trajectories that follow the flow direction so that $p(\theta) = \delta(\theta)$ and hence

$$\langle R_{\text{point}}(\tau)\rangle_{\text{flow}} = \frac{\pi T}{2r^2}\int_0^{\infty} dv p(v)v\exp -\frac{1}{r^2}(v\tau - d)^2.$$
$$= R_{\text{flow}}(\tau). \qquad (8)$$

To judge the effectiveness of the TTLV in measuring the speeds of a population of random swimmers, $R_{\text{random}}(\tau)$ may be evaluated for a collection of swimmers with the same speed, v_0 [i.e., $p(v) = \delta(v - v_0)$]:

$$R_{\text{random}}(\tau) = \frac{\pi T v_0}{2r^2}\exp\left\{-\frac{1}{r^2}(v_0^2\tau^2 + d^2)I_0\left(\frac{2v_0 d\tau}{r^2}\right)\right. . \qquad (9)$$

Figure 2*a* shows $R_{\text{random}}(\tau)$ calculated from Eq. 9 for r/d ratios in the range 0.1 to 0.5. A bias of the cross-correlation function is evident towards values of $\tau < d/v_0$. This biasing is less pronounced with the smaller beams because of their improved resolution, and as r/d is reduced $R_{\text{random}}(\tau)$ simplifies to $R_{\text{flow}}(\tau)$, which is symmetrical for laminar flows. For $r/d < 0.1$, $R_{\text{random}}(\tau)$ is almost indistinguishable from $R_{\text{flow}}(\tau)$. Furthermore, if the beam radius is reduced until the beam passage time is negligible compared with the transit time between the beams, $R_{\text{flow}}(\tau)$ and hence $R_{\text{random}}(\tau)$ reduce to the transit time distribution, $p(\tau)$.

Improving the resolution of the TTLV by reducing the beam sizes, however, has the disadvantage of sampling fewer particles. The resolution therefore has to be compromised to ensure that satisfactory statistics are achieved by sampling large numbers of particles with reasonably sized beams. In the experiments described here a value of $r/d = 0.25$ is used, and at this value the difference between $R_{\text{random}}(\tau)$ and $R_{\text{flow}}(\tau)$ is very small. Both cross-correlation functions are noticeably broader than $p(\tau)$, however, as a result of the appreciable beam passage time. Fig. 2*b* compares $p(\tau)$, $R_{\text{random}}(\tau)$ and $R_{\text{flow}}(\tau)$ for this value of $r/d = 0.25$ and a rms spread in speeds equal to one-tenth of the mean value. The difference in particle trajectories for flow and random motion is only just apparent in the slight bias of $R_{\text{random}}(\tau)$ towards the origin, compared with $R_{\text{flow}}(\tau)$.

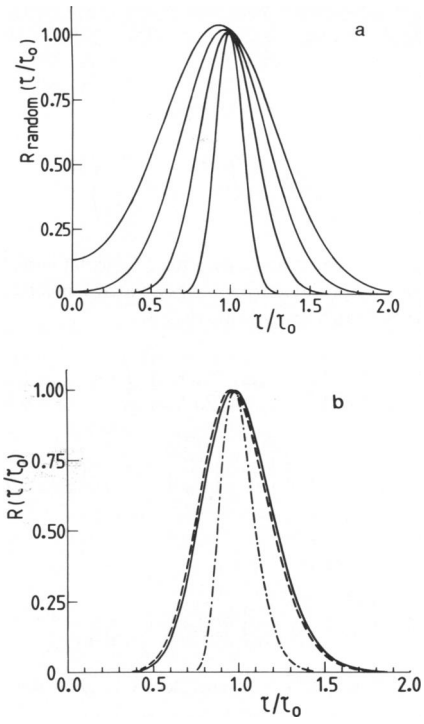

FIGURE 2 (*a*) $R_{\text{random}}(\tau/\tau_0)$ for an ensemble of swimmers of constant speed $[p(v) = \delta(v - v_0)]$ and beam-radius-to-beam-spacing ratios, $r/d = 0.125$, 0.25, 0.375, and 0.5. (*b*) Comparison between $R_{\text{random}}(\tau/\tau_0)$, $R_{\text{flow}}(\tau/\tau_0)$, and $p(\tau/\tau_0)$ for a population of swimmers with a normal distribution of speeds; $\sigma/v = 0.1$ and $r/d = 0.25$.

The transit-time distribution and cross-correlation functions of Fig. 2*b* were calculated under the assumption that speeds of the particles were normally distributed, i.e.

$$p(v) = \frac{1}{\sigma}\sqrt{\frac{2}{\pi}}\left(1 + erf\frac{\bar{v}}{\sqrt{2}\sigma}\right)^{-1}$$
$$\cdot\exp\frac{-1}{2\sigma^2}(v - \bar{v})^2 \text{ for } v \geq 0 \qquad (10)$$
$$= 0. \qquad \text{for } v < 0$$

Rikmenspoel and Herpen (1957) found that this distribution gave reasonable agreement with their observations of the motion of bull sperm. The functional forms of the cross-correlation functions for this distribution of speeds are given by

$$R_{\text{random}}(\tau) = K_0\int_0^{\infty} v\exp$$
$$-\left[\frac{1}{2\sigma^2}(v - \bar{v})^2 + \frac{1}{r^2}(v^2\tau^2 + d^2)\right]I_0\left(\frac{2vd\tau}{r^2}\right)dv \qquad (11)$$

$$R_{\text{flow}}(\tau) = K_0 \int_0^\infty v \exp - \left[\frac{1}{2\sigma^2}(v - \bar{v})^2 + \frac{1}{r^2}(v\tau - d)^2\right] dv \tag{12}$$

where

$$K_0 = \sqrt{\frac{\pi}{2}}\frac{T}{\sigma r^2}\left(1 + erf\frac{\bar{v}}{\sqrt{2}\sigma}\right)^{-1}.$$

$R_{\text{random}}(\tau)$ was evaluated numerically using a Gaussian-type formula with zeroes and weights calculated from the associated Laguerre polynomials. $R_{\text{flow}}(\tau)$ can be evaluated analytically to yield:

$$R_{\text{flow}}(\tau) = \frac{\pi}{2}\frac{T\bar{v}}{d^2\delta^2}\left(1 + erf\frac{\bar{v}}{\sqrt{2}\sigma}\right)^{-1}\left[\gamma\left(1 + erf\frac{\bar{v}}{\sqrt{2}\sigma}\gamma\right)\exp - \frac{1}{\sigma^2}\left(\frac{\tau}{\tau_0} - 1\right)^2 + \sqrt{\frac{2}{\pi}}\frac{\sigma}{\bar{v}}\exp - \left(\frac{d^2}{r^2} + \frac{\bar{v}^2}{2\sigma^2}\right)\right] \tag{13}$$

where

$$\tau_0 = \frac{d}{\bar{v}},\ \delta^2(\tau) = \left(\frac{r^2}{d^2} + \frac{2\sigma^2}{\bar{v}^2}\frac{\tau^2}{\tau_0^2}\right) \text{ and } \gamma(\tau) = \frac{r}{d\delta(\tau)}\left(1 + \frac{2\sigma^2}{\bar{v}^2}\frac{d^2}{r^2}\frac{\tau}{\tau_0}\right).$$

Typically $(d/r)^2 + (\bar{v}^2/2\sigma^2) \geq 5$, hence, as a very good approximation

$$R_{\text{flow}}(\tau) = \frac{\pi}{2}\frac{T\bar{v}\gamma}{d^2\delta^2}\left(1 + erf\frac{\bar{v}}{\sqrt{2}\sigma}\right)^{-1}\left(1 + erf\frac{\bar{v}\gamma}{\sqrt{2}\sigma}\right)\exp\frac{-1}{\delta^2}\left(\frac{\tau}{\tau_0} - 1\right)^2.$$

Furthermore, for the region of interest, $1/2 \leq \tau/\tau_0 \leq 2$, there is a very weak variation (<6%) in $\gamma(\tau)$ with τ. Hence, as a reasonable approximation,

$$R_{\text{flow}}(\tau) = \frac{\pi\bar{v}T\gamma(\tau_0)}{2d^2\delta(\tau)^2}\exp\frac{-1}{\delta(\tau)^2}\left(\frac{\tau}{\tau_0} - 1\right)^2. \tag{14}$$

The Effect of Particle Assymetry

The discussion has so far concerned swimmers of negligible size. Most motile micro-organisms, however, are of appreciable size and have an asymmetrical shape. In particular, bull sperm have large flat heads and are visible only if they swim in or near the plane perpendicular to the scattering vector (Harvey and Woolford, 1980). As they are also constrained to swim in a plane perpendicular to the incident beams in our apparatus, the bull sperm will be visible only in a small range of directions, θ, on either side of the line that is the intersection of this plane with the plane perpendicular to the scattering vector. Bull sperm are therefore intermediate between the two cases already outlined: randomly swimming point scatterers and point scatterers suspended in a flow. As discussed by Harvey and Woolford (1980), the range of directions over which the cell is visible decreases as the scattering angle increases. To simplify the analysis of the data, a scattering angle of 15° was chosen for these experiments so that the cells would only be visible for directions $\theta \leq 20°$. The data can therefore be expected to be well described by $R_{\text{flow}}(\tau)$ as given in Eq. 14. With the choice of beam radius and separation used here, $R_{\text{flow}}(\tau)$ and $R_{\text{random}}(\tau)$ are virtually indistinguishable, and either may be used to analyze the data.

In addition to the variation in scattered intensity with the direction of an asymmetric swimmer, there is a dependence upon the orientation of the cell about its center-of-mass. Temporal fluctuations in the scattered intensity may thereby arise should the cell possess internal degrees of freedom, and these can be expected to alter the form of the cross-correlation function from that derived for point scatterers. In the case of bull sperm, rotation of the head produces a predominant periodic modulation of the scattered intensity at twice the cell's rotational frequency (Harvey and Woolford, 1980). If the rotational and translational speeds of the cell are correlated, as suggested by Rikmenspoel et al. (1960), then the frequency of the intensity fluctuations will be proportional to the speed of the cell and a strong modulation of the cross-correlation function can be expected for an ensemble of cells with a narrow distribution of speeds.

To evaluate the exact form of the cross-correlation function it would be necessary to deduce the precise dependence of the scattered intensity upon the orientation of the cell. This dependence can be expected to be complex because of the large dimensions and asymmetrical shape of the cell. The scattering, however, is dominated by specular reflections from the flat surface of the head, and the temporal dependence of the reflected flash from a rotating cell may be modeled conveniently by the following expression:

$$I_f(t) = C_0 \exp\left[-\frac{1}{\beta^2}\sin^2(2\pi ft + \psi)\right]$$

where β determines the angular flash width seen at the detector, f is the rotational frequency, and ψ the initial orientation of the cell at $t = 0$. Assuming that the rotational frequency is equal to the translation speed divided by the pitch length of the cell's helical trajectory, l, i.e., $f = v/l$ (Rikmenspoel et al., 1960) then

$$I_f(t) = C_0 \exp\left[-\frac{1}{\beta^2}\sin^2\left(2\pi\frac{vt}{l} + \psi\right)\right]. \tag{15}$$

The intensity of the light scattered by a bull spermatozoon moving through the two beams of the TTLV is therefore

$$I_{is}(t) = \frac{C_0}{r^2}\exp - \left\{\frac{1}{\beta^2}\sin^2\left(\frac{2\pi vt}{l} + \psi\right) + \frac{2}{r^2}\left|vt + x_0 \pm \frac{d}{2}\right|^2\right\}, \tag{16}$$

where $i = 1, 2$. The cross-correlation between the intensities is

$$\begin{aligned}
R_{\text{sperm}}(\tau) &= \int_{-\infty}^{\infty} dt I_{1s}(t) I_{2s}(t + \tau) \\
&= \frac{r}{2v}\int_{-\infty}^{\infty} d\xi I_{1s}\left(\frac{r\xi}{2v} - \frac{\tau}{2} - \frac{x_0}{v}\right) I_{2s}\left(\frac{r\xi}{2v} + \frac{\tau}{2} - \frac{x_0}{v}\right) \\
&= \frac{C_0^2}{2vr^3}\exp - \frac{1}{r^2}\{|\mathbf{v}\tau - \mathbf{d}|^2 + 4y_0^2\} \\
&\quad \int_{-\infty}^{\infty} d\xi\, e^{-\xi^2} I_f\left(\frac{r\xi}{2v} - \frac{\tau}{2} - \frac{x_0}{v}\right) I_f\left(\frac{r\xi}{2v} + \frac{\tau}{2} - \frac{x_0}{v}\right) \\
&= R_{\text{point}}(\tau) C_0^2 \frac{e^{-1/\beta^2}}{\sqrt{\pi}} \int_{-\infty}^{\infty} d\xi \exp \\
&\quad - \left\{\xi^2 - \frac{1}{\beta^2}\cos 2\left[\psi + \frac{\pi}{l}(r\xi - 2x_0)\right]\cos\left(\frac{2\pi v\tau}{l}\right)\right\}.
\end{aligned} \tag{17}$$

In the above integration the following change of variable (from t to ξ) has been made: $t = (r\xi - v\tau - 2x_0)/(2v)$. The many-sperm cross-correlation function is an average of Eq. 17 over velocity $\mathbf{v}$, initial position $\mathbf{r}_0$ and initial observation ψ:

$$\langle R_{\text{sperm}}(\tau)\rangle = \frac{C_0^2\, e^{-1/\beta^2}}{\sqrt{\pi}} \iiint \mathbf{dr_0}\, d\psi\, d\mathbf{v}\, p(\mathbf{v})\, R_{\text{point}}(\tau) \int_{-\infty}^{\infty} d\xi \exp - \left\{\xi^2 - \frac{1}{\beta^2}\cos 2\left[\psi + \frac{\pi}{l}(r\xi - 2x_0)\right]\cos\frac{2\pi v\tau}{l}\right\}$$

$$= \frac{C_0^2 e^{-1/\beta^2}}{2r^3} \int \mathrm{d}\mathbf{v}\, p(\mathbf{v}) \int_{-v\tau}^{v\tau} \mathrm{d}x_0 \int_{-\infty}^{\infty} \mathrm{d}y_0 \frac{1}{v} \exp - \frac{1}{r^2}$$

$$\cdot \left(|\mathbf{v}\tau - \mathbf{d}|^2 + 4y_0^2 \right) \int_{\infty}^{\infty} \mathrm{d}\xi \int_0^{2\pi} \mathrm{d}\psi \ \exp$$

$$- \left\{ \xi^2 - \frac{1}{\beta^2} \cos 2 \left[\psi + \frac{\pi}{l} (r\xi - 2x_0) \right] \cos \frac{2\pi v\tau}{l} \right\}$$

$$= \frac{C_0 \pi^2 e^{-1/\beta^2} T}{r^2} \int \mathrm{d}\mathbf{v}\, p(\mathbf{v}) \exp - \frac{1}{r^2} |\mathbf{v}\tau - \mathbf{d}|^2$$

$$\cdot I_0 \left(\frac{1}{\beta^2} \cos \frac{2\pi v\tau}{l} \right)$$

$$= \frac{C_0^2 \pi^2 e^{-1/\beta^2} T}{r^2} \int_0^{\infty} v \mathrm{d}v p(v) \int_0^{2\pi} \mathrm{d}\theta q(\theta) \exp$$

$$- \frac{1}{r^2} |\mathbf{v}\tau - \mathbf{d}|^2 I_0 \left(\frac{1}{\beta^2} \cos \frac{2\pi v\tau}{l} \right) \quad (18)$$

where $p(v)$ is the distribution of sperm speeds and $q(\theta)$ is the apparent distribution of directions.

In the case of an ensemble of sperm cells with a very narrow distribution of speeds, i.e., $p(v) = \delta(v - v_0)$

$$\langle R_{\text{sperm}}(\tau) \rangle = \frac{C_0^2 \pi^2 e^{-1/\beta^2} T v_0}{r^2} I_0 \left(\frac{1}{\beta^2} \cos \frac{2\pi v_0 \tau}{l} \right)$$

$$\int_0^{2\pi} \mathrm{d}\theta q(\theta) \exp \frac{-1}{r^2} (v^2\tau^2 - 2vd\tau \cos\theta + d^2)$$

$$= C_0^2 2\pi e^{-1/\beta^2} I_0 \left(\frac{1}{\beta^2} \cos \frac{2\pi v_0 \tau}{l} \right) \langle R_{\text{point}}(\tau) \rangle \quad (19)$$

$\langle R_{\text{sperm}}(\tau) \rangle$ is thus equal to the point-scatterer cross-correlation function strongly modulated at the flash frequency $2v_0/l$.

In practice all sperm samples show a relatively large spread in speeds. For a sample with normally distributed speeds (i.e. $p(v)$ as given in Eq. 10)

$$\langle R_{\text{sperm}}(\tau) \rangle = K \int_0^{\infty} v \mathrm{d}v\, I_0 \left(\frac{1}{\beta^2} \cos \frac{2\pi v\tau}{l} \right)$$

$$\exp - \left\{ \frac{-1}{2\sigma^2} (v - \bar{v})^2 + \frac{1}{r^2} (v^2\tau^2 + d^2) \right\}$$

$$\int_0^{2\pi} \mathrm{d}\theta q(\theta) \exp \left(\frac{2vd\tau \cos\theta}{r^2} \right) \quad (20)$$

where

$$K = \frac{C_0^2 \sqrt{2\pi^3}\, T e^{-1/\beta^2}}{\sigma r^2} \left\{ 1 + erf \frac{\bar{v}}{\sqrt{2}\sigma} \right\}^{-1}.$$

As discussed earlier, the apparent directional distribution, $q(\theta)$, for bull sperm is intermediate between the limits $p_{\text{random}}(\theta) = 1/(2\pi)$ and $p_{\text{flow}}(\theta) = \delta(\theta)$. The experimentally determined cross-correlation must therefore be intermediate between the limits:

$$R_{\text{sperm,random}}(\tau) = K \int_0^{\infty} v \mathrm{d}v I_0 \left(\frac{1}{\beta^2} \cos \frac{2\pi v\tau}{l} \right) I_0 \left(\frac{2vd\tau}{r^2} \right)$$

$$\exp - \left\{ \frac{1}{2\sigma^2} (v - \bar{v}) + \frac{1}{r^2} (v^2\tau^2 + d^2) \right\} \quad (21)$$

and

$$R_{\text{sperm,flow}}(\tau) = K \int_0^{\infty} v \mathrm{d}v I_0 \left(\frac{1}{\beta^2} \cos \frac{2\pi v\tau}{l} \right) \exp$$

$$- \left\{ \frac{1}{2\sigma^2} (v - \bar{v})^2 + \frac{1}{r^2} (v\tau - d)^2 \right\}$$

$$= \frac{2Kd^2\delta^2(\tau)}{\pi \bar{v} T} R_{\text{flow}}(\tau) \int_0^{\infty} v \mathrm{d}v I_0 \left(\frac{1}{\beta^2} \cos \frac{2\pi v\tau}{l} \right)$$

$$\cdot \exp \left\{ - \alpha^2(\tau) \left(\frac{v\tau}{l} - \frac{\gamma(\tau)\bar{v}}{\alpha(\tau)\sqrt{2}\sigma} \right)^2 \right\} \quad (22)$$

where $R_{\text{flow}}(\tau)$ is the point scatterer cross-correlation function (Eq. 14) and

$$\alpha(\tau) = \frac{l\tau_0 \bar{v} \delta(\tau)}{r\tau \sqrt{2}\sigma}.$$

$R_{\text{sperm,flow}}(\tau)$ is equal to the point-scatterer cross-correlation function modulated at the flash frequency $2v/l$. The modulation decays rapidly at a rate determined by the spread in speeds. Fig. 3 shows $R_{\text{sperm,flow}}(\tau)$ for a range of values of $\sigma/\bar{v}$ between 0 and 0.1 and a value of $\beta = 1/6$. Almost identical graphs are outlined for $R_{\text{sperm,random}}(\tau)$. Typically sperm samples have an rms spread in speeds >10% of the mean value. At this level of dispersion, the modulation of the correlation function becomes undetectable and hence the flashing phenomenon characteristic of swimming bull sperm can be expected to have no effect on the TTLV technique.

METHODS

The transit-time laser velocimeter described in the previous section has been built in a variety of configurations, shown schematically in Fig. 4. The simplest configuration is depicted in Fig. 4*a*. Two identical, intersecting beams were formed by splitting the output beam of a 3 mW HeNe laser with a beam-splitting cube. The beam cross-over was at the focal point of a converging lens (f = 5 cm). The beams emerged from the lens convergent and parallel, separated by <0.1 mm in the horizontal plane. The scattering cell was positioned over the beam waists and surrounded by a heated waterjacket. The beam separation and waist sizes were

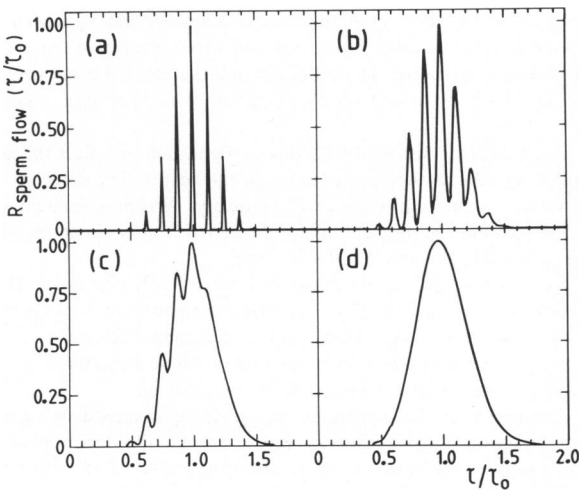

FIGURE 3 $R_{\text{sperm, flow}}(\tau/\tau_0)$ for a population of bull sperm with normal distributions of speed; ratio of beam-radius-to-beam-spacing, r/d = 0.25; ratio of beam-radius-to-pitch length of sperms' helical trajectory, r/l = 1; relative rms spread in speeds, $\sigma/\bar{v}$, = 0.0 (*a*), 0.025 (*b*), 0.05 (*c*), 0.1 (*d*); flash width β = ⅙ (see text).

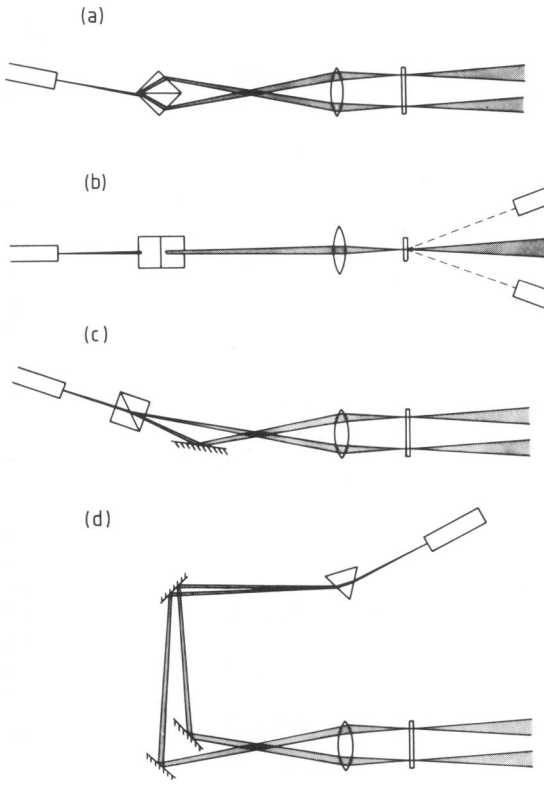

FIGURE 4 Various versions of the transit time apparatus used for measuring the velocity of spermatozoa. (*a*) Identical beams with a single detector (top view): HeNe laser, cube beamsplitter, lens (f = 5 cm) and scattering cell. (*b*) Identical beams with two detectors (side view): HeNe laser, cube beamsplitter, lens, scattering cell, and detectors. (*c*) Orthogonally polarized beams with two detectors (top view): HeNe laser, Wollaston prism, mirror, lens, and scattering cell. (*d*) Differently colored beams with two detectors (top view): argon ion laser, dispersion prism, mirrors, and beamsplitter, lens, and scattering cell.

variable, typical values were 55 μm for the beam separation and 25 μm for the beam diameter. The optimum choice of beam size and separation is a compromise between large beam size and small separation (to ensure good statistics and shorter data collection times) and small beam size and large separation (to ensure good collimation of the particles' trajectories).

A single detector was used with this configuration to collect the light scattered by cells as they passed through the beams. The detector was oriented at a scattering angle of 8° vertically; vertical alignment was desirable to minimize the light intensity received from sedimenting dead spermatozoa (Harvey and Woolford, 1980).

The detected signal was autocorrelated in a HP3721 correlator (Hewlett-Packard Co., Palo Alto, CA). The major component of the autocorrelation function was a single beam passage component centred at $\tau = 0$. The other component arose from those cells whose trajectories passed through both beams (the cross-correlation component).

A refinement of this apparatus incorporating a second detector is shown in Fig. 4*b*. The two detectors were oriented in the vertical plane on opposite sides of the beams at equal scattering angles of 15°. With two such detectors it is possible, in principle, to obtain the cross-correlation peak without the single-beam passage component. This was achieved by placing pinholes in the image plane of the lens in each of the detectors to ensure that each detector received scattered light from only one of the beams. The two signals formed in this manner were then cross-correlated in the HP3721 correlator. With the aid of a second correlator two cross-correlation functions were collected simultaneously from different groups of cells moving in opposite directions.

The above system was further improved by the use of orthogonally polarized beams. As shown in Fig. 4*c* this was achieved by splitting the output beam of a HeNe laser with a Wollaston prism. Polarizers were incorporated into the detection system to improve the discrimination between light scattered from the two beams.

The fourth experimental arrangement involving beams of different wavelengths is shown in Fig. 4*d*. The output beam of a 4 W Argon ion laser was split by a dispersion prism into its various component wavelengths, two of which (488 and 514.5 nm) were selected to form the TTLV. Interference filters were used in the detection system in this case to distinguish between the beams.

The correlator typically took twenty minutes to form each correlation function. The correlator was interfaced to a Computer Automation LSI-2 mini-computer (Computer Automation Inc., Irvine, CA), for data storage and analysis.

The mean speed and standard deviation can be deduced from the cross-correlation functions provided that the beam separation and waist size are known. These were measured using a rotating chopper to interrupt the twin beams while they were incident on a light-sensitive diode. Using the correlator in signal recovery mode, the eclipsed light intensity as a function of time was recorded and transferred to the computer for analysis.

To operate the chopper it was necessary to remove the scattering chamber and waterbath and measure the beam separation and radii in air. Because the beams are parallel, their separation measured in this manner is equal to their separation when in water. Refraction of the beam wave-fronts at the interface between the two media, however, causes a change in the size and position of the beam waists. If d is the distance from the interface to the beam waist in water, r is the beam waist in water, and d_a and r_a are the same quantities in the air, then it can be shown (see Appendix) that

$$d = \frac{d_a}{n}\left[1 + \left(\frac{\lambda d_a}{\pi r_a^2}\right)^2\right]\left[1 + \left(\frac{\lambda d_a}{n\pi r_a^2}\right)^2\right]^{-1}$$

and $r^2 = r_a^2\,(nd)/d_a)$. In these experiments $(\lambda d_a)^2/(\pi r_a^2)^2 \gg 1$, hence $d \simeq nd_a$, the apparent depth correlation for paraxial rays, and $r \simeq nr_a$.

The transit-time technique requires that cells swim only in a direction perpendicular to that of the beams. This was accomplished by taking advantage of the pronounced preference of the spermatozoa for swimming next to the walls of the glass cuvettes (Rothschild, 1963). The scattering cell used in these experiments was designed to optimize this effect, and is similar in design to the short pathlength cell described by Woolford (1981).

Semen was obtained from the New Zealand Dairy Board Artificial Breeding Centre at Newstead. Bulls were of Jersey of Freisan breeds. Sample handling has been discussed elsewhere (Woolford, 1981).

Semen diluted with Caprogen extender was supplied at a concentration of 10^8 sperm/ml. Subsequent dilution immediately before the experiments, again with the extender, reduced the concentration to 10^7 sperm/ml. Experiments were usually performed within 8 h of sperm collection.

RESULTS

Figs. 5, 6, and 7 show the results achieved with the versions of the TTLV apparatus shown in Figs. 4*a*, *b*, and *d*, respectively.

The autocorrelation function of the light scattered from both beams into a single detector appears in Fig. 5. The cross-correlation component occurs as a broad peak centred at τ = 400 ms and corresponds to an average translational velocity of 150 μm/s. Typically, the beam radius is one-quarter of the beam spacing and only 15% of

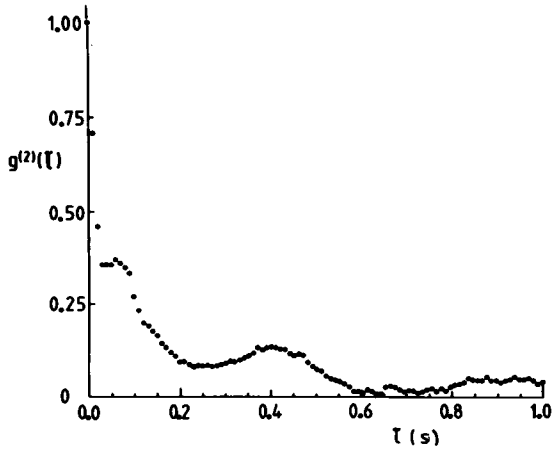

FIGURE 5 The auto-correlation function of the light scattered by bull spermatozoa from identical beams into a single detector. This auto-correlation function was collected using the apparatus of Fig. 4*a*; r = 13 μm, d = 60 μm and $\bar{v}$ = 150 μm/s, at a concentration of 10^7 cells/ml and a temperature of 37°C.

those cells swimming through one beam also swim through the other. Consequently the auto-correlation function is dominated by the single-beam passage component. The persistence of this single-beam component, due to the dead sperm, makes it difficult to recover the cross-correlation component.

The presence of oscillations in the light scattered by swimming bull spermatozoa is indicated by the small peak at τ = 0.06 s corresponding to an average rotational frequency of 8.3 Hz (this assumes that the cells flash twice per revolution).

Fig. 6 shows a typical cross-correlation function of the light scattered from identical beams into separate detectors. Although a marked improvement has been achieved

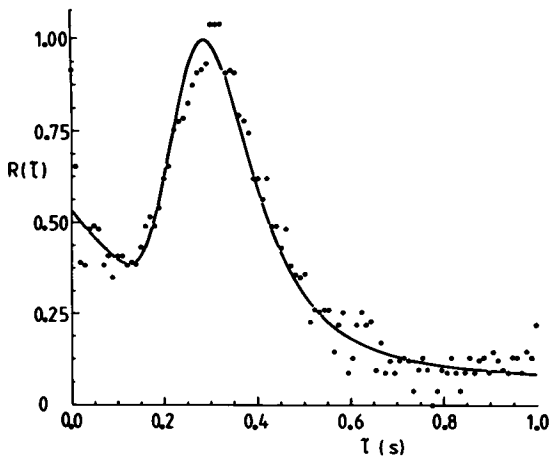

FIGURE 6 The cross-correlation function of the light scattered by bull spermatozoa from identical beams into separate detectors (. . . .), together with the best fit of R_{flow} (τ) (—). This cross-correlation function was obtained using the apparatus of Fig. 4*b*; r = 13.4 μm, d = 55.5 μm, $\bar{v}$ = 168 μm/s, σ = 40 μm/s, at a concentration of 10^7 cells/ml and a temperature of 42°C.

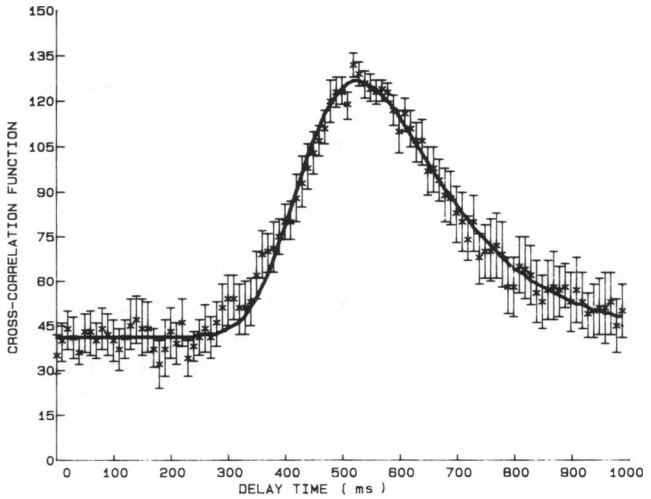

FIGURE 7 The average cross-correlation function of the light scattered from differently colored beams by bull spermatozoa (×), together with the best fit of $R_{flow}(\tau)$ (—). Associated error bars for each data point are shown. This correlation function was obtained using the apparatus of Fig. 4*d*; r = 16.2 μm, d = 90.1 μm, $\bar{v}$ = 157 μm/s, σ = 33.0 μm/s, at a concentration of 10^7 cells/ml and a temperature of 39°C.

by comparison with the results shown in Fig. 5 for a single detector, a small, residual, single-beam component still remains. This component is generated when stray light from one beam enters the detection system of the other beam. The amount of stray light can be minimized but not completely eliminated because of the proximity of the two beams and the size of the pinholes needed to obtain a reasonable signal level (50 μm in these experiments).

This problem was overcome when the beams were either orthogonally polarized or differently colored. Results achieved with the differently colored beams were essentially the same as those achieved with the orthogonally polarized beams. Partial depolarization of the light scattered by bull spermatozoa, however, required the use of 50

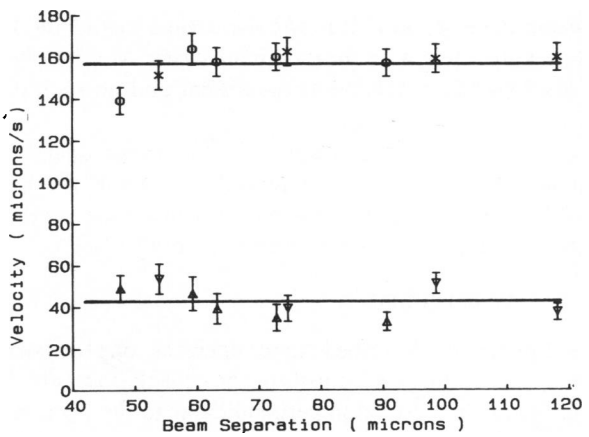

FIGURE 8 Mean speeds (0, ×) and rms spreads in speed (Δ, ∇) for two bulls, as determined by least-squares curve fitting, over a range of beam spacings. Error bars for each measurement are indicated, as are the average values of the mean speed and rms spread in speed (—).

μm pinholes with the polarized beams apparatus. These pinholes were unnecessary with the two-color apparatus, and consequently the detection system was easier to align in this case. A typical example of the results obtained with the two-color apparatus of Fig. 4*d* is shown in Fig. 7 together with the best fit of $R_{flow}(\tau)$ as given by Eq. 14.

Comparison of the theoretical cross-correlation functions of Eqs. 11 and 14 and the experimental data was performed by least-squares curve fitting using the Gauss-Newton algorithm on the CAI LSI-2 mini-computer. Typical best fits are shown in Figs. 6 and 7. (An exponential background has been included in the fit of Fig. 6 to allow for the residual single-beam passage component.) This curve fitting procedure enabled the mean and standard deviation of the speed distribution to be extracted from the experimental cross-correlation function.

Fig. 8 depicts the results of various measurements, at different beam separations, of the mean speed and standard deviation in speed of bull spermatozoa from two different animals. Following normal procedure the semen samples were diluted with the Caprogen extender. Caffeine, at a concentration of one part in a thousand, was added to the extender to stimulate motility in a uniform manner. The sample was maintained at a temperature of 39°C for the duration of the assay. At each beam spacing a different fraction of one of the two ejaculates was used.

Beam separations in the range 55 to 120 μm were found to be satisfactory for the determination of the velocity parameters. Longer delay times and consequently lengthy data collection times were required if the beam separation exceeded 120 μm. At separations of 50 μm or less, estimates of the mean speed were consistently below the average. Cross-correlation functions collected at these short beam separations appeared to contain an additional component centered at $\tau = 0$, which may have been due to particles larger than the beam separation sedimenting through both beams simultaneously. Because the functional form of this additional term was unknown, it was not possible to incorporate it in the theoretical model and thus obtain agreement with the data in all cases. At larger beam separations this component was absent and no such difficulties were encountered.

To conclude, the constancy of the mean speed and standard deviation in speed for separations in the range 55–120 μm indicates that bull spermatozoa swim in straight trajectories for distances exceeding 120 μm.

DISCUSSION

The apparatus described here operates on the simple principle of timing the transits of the cells that traverse two laser beams in a direction perpendicular to the beam axes. This technique can be applied to any collection of organisms satisfying the requirement that the correlation function be formed only from light scattered by organisms moving perpendicular to the beams. In the case of bull spermatozoa this requirement is satisfied in two ways. First, those cells that traverse both beams at an oblique angle scatter very little light to the detector as a result of the previously described orientational effect (Harvey and Woolford, 1980). Second, as discussed earlier, bull spermatozoa show a strong tendency to swim on the walls of the cuvette, and, in the geometry chosen here, the walls are normal to the beams. The technique could thus be used to study the motion of any organism that displays such behavior, regardless of its shape. In addition, for cells displaying a strong flashing effect, such as many types of mammalian spermatozoa, the technique could be used in a cuvette far from the walls. This would make comparison of the swimming motion close to walls with that in the body of the cuvette possible.

In conclusion, the TTLV provides a reliable method for the direct measurement of the translational velocity distribution of bull spermatozoa that, unlike the widely used single-beam laser light-scattering techniques, is unaffected by the rotational motion of the organism. The method thus complements the single-beam technique for the study of spermatozoan and microbial motility.

APPENDIX

Mode-Matching Laser Beams in Dielectric Media of Different Refractive Indices

The propagation of a Gaussian laser beam is governed by the equations for the beam radius

$$r^2(z) = r_0^2\left[1 + \left(\frac{\lambda z}{\pi r_0^2}\right)^2\right] \tag{A1}$$

and the radius of curvature of the wavefront

$$R(z) = z\left[1 + \left(\frac{\pi r_0^2}{\gamma z}\right)^2\right] \tag{A2}$$

where r_0 is the minimum beam radius, i.e., beam radius at the waist. z is the distance along axis of propagation from beam waist.

If such a beam with a waist r_{01} situated at d_1 passes from a dielectric medium of refractive index, n_1, to another of refractive index, n_2, refraction of the beam wavefronts occurs at the interface. This will change both the position and size of the beam waist (to d_2 and r_{02}). The change in radius of curvature of the beam wavefront at the interface is given by

$$R_1(d_1) = \frac{R_2(d_2)}{n}, \text{ where } n = \frac{n_2}{n_1}. \tag{A3}$$

From (A1) and (A2),

$$R(z) = \frac{\pi^2 r_0^2 r^2(z)}{\lambda^2 z}. \tag{A4}$$

At the interface both beams must have equal radii, hence

$$r_1^2(d_1) = r_2^2(d_2) \tag{A5}$$

and from Eqs. A3 and A4

$$\frac{r_{01}^2}{d_1} = \frac{r_{02}^2}{nd_2}. \tag{A6}$$

Hence, from Eqs. A1, A5, and A6

$$r_{02}^2 = r_{01}^2\left[1 + \left(\frac{\lambda d_1}{\pi r_{01}^2}\right)^2\right]\left[1 + \left(\frac{\lambda d_1}{n\pi r_{01}^2}\right)^2\right]^{-1}$$

and

$$d_2 = \frac{d_1}{n}\left[1 + \left(\frac{\lambda d_1}{\pi r_{01}^2}\right)^2\right]\left\{1 + \left(\frac{\lambda d_1}{n\pi r_{01}^2}\right)^2\right\}^{-1}.$$

Typically, $\lambda = 633$ nm, $d = 1$ cm, $r_{01} = 10\ \mu$m. Thus $(\lambda d_1)/(\pi r_{01}^2) = 406 \gg 1$; hence $r_{02} \simeq n r_{01}$ and $d_2 \simeq n d_1$, which is the apparent depth correction.

REFERENCES

Bergé, P., B. Volchine, R. Billard, and A. Hamelin. 1967. Mise en évidence du movement propre de micro-organisms vivants grâce â l'étude de la diffusion inélastique de lumière. *C.R. Acad. Sci. Ser. D.* 265:889–892.

Craig, T., F. R. Hallett, and B. Nickel. 1979. Quasi-electric light scattering spectra of swimming spermatozoa. Rotational and translational effects. *Biophys. J.* 28:457–472.

Cummins, H. Z. 1977. Intensity fluctuation spectroscopy of motile organisms. *In* Photon Correlation Spectroscopy and Velocimetry. H. Z. Cummins and E. R. Pike, editors. Plenum Publishing Corp., New York.

Durrani, T. S., and C. A. Greated. 1975. Spectral analysis and cross-correlation techniques for photon counting measurements on fluid flows. *Applied Optics* 14:778–786.

Durrani, T. S., and C. A. Greated. 1977. Laser Systems in Flow Measurement. Plenum Publishing Corp., New York.

Harvey, J. D., and M. W. Woolford. 1980. Laser light-scattering studies of bull spermatozoa. I. Orientational effects. *Biophys. J.* 31:147–156.

Kugler, H. P. 1979. Recent results in rocket exhaust anemometry. *Physica Scripta.* 19:447–452.

Lading, L. 1976. The time-of-flight anenometer. *AGARD (Advis. Group Aerosp. Res. Dev.) Conf. Proc.* 193:Paper 23.

Papoulis, A. 1965. Probability, Random Variables, and Stochastic Processes. McGraw-Hill, Inc., New York.

Rikmenspoel, R., and G. Van Herpen. 1957. Photoelectric and Cinematographic Measurements of the Motility of Bull Sperm Cells. *Phys. Med. Biol.* 2:54–63.

Rikmenspoel, R., G. van Herpen, and P. Eijkhout. 1960. Cinematographic Observations of the movements of bull sperm cells. *Phys. Med. Biology* 5:167–181.

Rothschild, Lord. 1963. Non-random distribution of bull spermatozoa in a drop of sperm suspension. *Nature (Lond.)* 198:1221–1222.

Schodl, R. 1976. The laser dual focus flow velocimeter. AGARD (*Advis. Group Aerosp. Res. Dev.*) *Conf. Proc.* 193:Paper 21.

Woolford, M. W. 1981. Laser light scattering as a probe of bovine sperm motility. Ph.D. Dissertation, University of Waikato, New Zeland.